Structure and Bonding in Magnesium Difluoride Clusters: The $(MgF_2)_n$ ($n = 2-3$) Clusters

E. Francisco,* A. Martín Pendás, and A. Costales

Departamento de Química Física y Analítica, Facultad de Química, Universidad de Oviedo, E-33006 Oviedo, Spain

Received: June 19, 2001; In Final Form: October 30, 2001

Hartree−Fock (RHF) and second-order Møller−Plesset (MP2) first principles calculations have been performed to study the structures, stabilities, harmonic vibrational frequencies, and bonding properties of MgF_2 dimers and trimers, complementing our previous work (*J. Phys. Chem.* **2001**, *105*, 4126) on the MgF_2 monomer. The less energetic isomers found for $(MgF_2)_2$ and $(MgF_2)_3$ are the bridged F−(Mg_2F_2)−F (D_{2h}) and F−MgF_2-MgF_2Mg−F (D_{2d}) structures, respectively. A new C_s trimer structure has been found and characterized. Correlation energy corrections increase the Mg−F distances by 1.2−1.4% and do not modify appreciably the Mg−F−Mg and F−Mg−F angles. The dissociation energy per MgF_2 unit (DE) of $(MgF_2)_n$ increases with n. MP2 frequencies for the $(MgF_2)_2$ D_{2h} isomer are around 1.0% lower than their RHF equivalents. The whole set of computed frequencies for $(MgF_2)_n$ has allowed us to perform a critical analysis of the experimental vibrational data, where some spectral assignments remained uncertain. The atoms in molecules analysis of the electron density reveals that $(MgF_2)_n$clusters are highly ionic, with almost nominal net atomic charges ($q_{Mg} \simeq +1.8|e|$ and $q_F \simeq -0.9|e|$). Our previous polarizable-ions model accounts fairly well for the properties of these clusters, rationalizing the energy ordering of trimers in a physically sound way.

I. Introduction

High-temperature vapors of the alkaline earth dihalides solids are well-known to contain appreciable amounts of monomers (AX_2), dimers [$(AX_2)_2$], trimers [$(AX_2)_3$], and higher polymeric species.[1] The monomers have been investigated both theoretically and experimentally to some extent, but almost nothing is experimentally known about the structure of dimers and trimers. Some indirect conclusions about dimers may be extracted through the analysis of the vibrational infrared (IR) and Raman spectra of the vapors trapped in solid matrixes.[2] However, the simultaneous presence of several species makes the unambiguous assignment of the observed bands a rather difficult task.

On the theoretical front, the $(MgF_2)_n$ clusters have been studied using atomistic[3−6] and quantum-mechanical methods.[7−10] In the dimer, Gigli[3] found that the double-bridged (D_{2h}) and triple-bridged (C_{3v}) structures are local minima on the potential energy surface given by the polarizable-ion model of Rittner.[11] The D_{2h} isomer was found to be lower in energy than the triple-bridged isomer. Molecular orbital calculations confirmed these results,[7−10] and after scaling the restricted Hartree−Fock (RHF) computed frequencies of the D_{2h} isomer, the calculations support the experimental spectral identification of this structure in magnesium dihalide vapors reported by Lesiecki and Nibler.[2] As the trimer is concerned, we are not aware of any ab initio study other than the RHF molecular orbital calculations by Axten et al.[10] and by Ystenes et al.[8] in the double-bridged (D_{2d}) isomer. As far as we know, the structure and relative stabilities of other isomers of this cluster have not been studied using molecular orbital methods. Moreover, in some of the above calculations, the harmonic vibrational spectra are obtained at the optimized RHF geometries, taking into account correlation effects at a second-order Møller−Plesset (MP2) level. In other cases, the spectra are obtained at the RHF level at MP2 optimized geometries. In none of these works is the D_{2d} isomer of $(MgF_2)_3$ is studied beyond the RHF approximation. A unified vision of the structure and properties of these cluster is, therefore, lacking.

As in our previous work devoted to the MgF_2 monomer (referred to as paper I in the following),[12] the present article reports results from first-principles calculations on the geometry, relative stability, vibrational spectra, and chemical bonding of selected isomers of the $(MgF_2)_n$ ($n = 2-3$) systems. Basis set and correlation effects in the monomer have been fully studied in paper I, which is used here as a guide to select a small number of relevant basis sets and levels of calculation that were formerly shown to saturate reasonably well the different observables under study. The reader is referred to paper I for a full account of these details.

Our main goal in this work is 2-fold. First, we will characterize the lowest energy isomers of the $(MgF_2)_n$ ($n = 2-3$) clusters and critically analyze the experimentally assigned vibration frequencies. Second, we will examine the change of the geometrical and bonding properties with the cluster sizes. From these analyses, it will become clear that all of the isomers studied here are extremely ionic species with structures completely determined by the polarizable-ions model (PIM) introduced in paper I. The usefulness of such an approach is here emphasized by showing how the dipole−dipole interactions among the fluorides in the trimer stabilize the D_{2d} ground-state isomer against the planar D_{3h} one. The analysis of the electron density and Laplacian fields through the atoms in molecules (AIM) theory of Bader and co-workers,[13] shows that the Mg and F species are almost perfectly transferable among all of the isomers and that the slight differences among them are mostly due to the dependence of the AIM magnitudes on the interatomic distances. We will also find how the small differences among the Mg^{2+} and F^- ions in the different clusters correlate rather well with the coordination index of the ion. The

* To whom correspondence should be addressed.

10.1021/jp012347+ CCC: $22.00
Published on Web 12/08/2001

AIM analysis has also cleanly uncovered that the structure of the $(MgF_2)_3$ C_s isomer may be interpreted as an almost perfect juxtaposition of the C_{3v} and D_{2d} isomers of the dimer. This fact suggests a tendency of these very ionic systems to build up big structures using just a small number of building blocks. All our conclusions are in agreement with the general predictions of paper I, and it seems plausible to expect that the PIM could be able to explain the structures and energetic ordering of a number of $(MgF_2)_n$ isomers at n values well above those that the present ab initio methods are able to deal with.

The structure of the paper is as follows. In section II, we describe the methods used in the work and the calculations performed. Particular attention is paid to the generation of starting cluster configurations by means of a Monte Carlo atomistic recipe. In section III, we present the lowest energy isomers found for the two stoichiometries here studied and discuss their geometries, energetic properties, and harmonic vibrational spectra. The nature of the interactions in the light of the AIM framework is presented in section IV. Finally, in section V, we comment on the expected generality of the insights that our approach provides for these very ionic clusters.

II. Theoretical Methods and Calculations

It is well-known that the number of stable isomers for clusters of a given stoichiometry increases exponentially with the number of monomers. It is therefore very important to discover reasonable topologies to be used as starting points in ab initio minimizations. In this work, a preliminary selection of isomers prior to ab initio computations has been guided by a three-step procedure. First, the electron gas model (EGM) of Gordon and Kim[14,15] was used to derive short-range interatomic potentials for the Mg−Mg, Mg−F, and F−F pairs. Second, the Monte Carlo growing strategy developed by Phillips et al.[16] was employed to obtain 1000 initial configurations for $(MgF_2)_n$ (n = 2−3). These geometries were subsequently optimized by means of a Powell's quadratically convergent method. Finally, our prescription's third step orders the resulting optimal structures by increasing energies. Several physical and graph-theoretical discriminating indices are used to automatically classify the final configurations into physically different species.

After this procedure, only three different isomers were found for $(MgF_2)_2$. The global minimum was found to be a double-bridged D_{2h} structure. The first excited isomer turned out to be a C_{3v} triple-bridged molecule, and the third structure, rather higher in energy than the other two, showed a C_{2v} configuration and will not be considered here. The molecular graphs of these and all of the other clusters discussed in this work are found in Figure 1. The D_{2h} and C_{3v} forms coincide with those obtained by Gigli,[3] using the polarizable-ion model of Rittner,[11] and also with those investigated by Ramondo et al.,[7] Axten et al.,[10] and Ystenes et al.[8] using molecular orbital methods.

As $(MgF_2)_3$ is concerned, 11 different isomers were located with the atomistic procedure. The more stable ones are a six-member planar D_{3h} ring form, a double-bridged D_{2d} geometry, and an interesting nonplanar C_s structure. These three isomers, very close in energy, are considerably more stable than the other eight and will be the only ones discussed here. The D_{3h} and D_{2d} forms were also found by Martin[4] in his simulation of $(MX_2)_n$ clusters using an atomistic method very similar to that used by Gigli.[3] The D_{2d} structure has even been studied with molecular orbital methods.[10] However, as far as we known, the D_{3h} and C_s isomers have never been investigated with ab initio methodologies.

Optimized configurations of the selected isomers coming from the atomistic simulations were used as starting points in the RHF and MP2 ab initio minimizations. Only the singlet ground electronic states have been considered. No MP4 calculations have been attempted, because MP4 correlation corrections were found in paper I to be very similar to those at the MP2 level. As also shown in paper I, large polarized basis sets are needed to saturate the atomic and molecular dipoles of these species, so we have only used basis sets of quality greater than triple-ζ in the valence segment. In this way, TZV is the (13s/9p)/[6s/5p] basis set of McLean and Chandler[17] with a contraction scheme (631111/42111) in the case of Mg and the (11s/6p)/[5s/3p] basis set of Dunning[18] with a contraction scheme (62111/411) for F. The TZV(1d) basis set is obtained by augmenting the TZV basis with a d-type function (α_d(Mg) = 0.234, α_d(F) = 1.62). Finally, the TZV(1d)+ basis set is the TZV(1d) basis with a one diffuse sp shell of exponents (α_{sp}(Mg) = 0.0146, α_{sp}(F) = 0.1076).

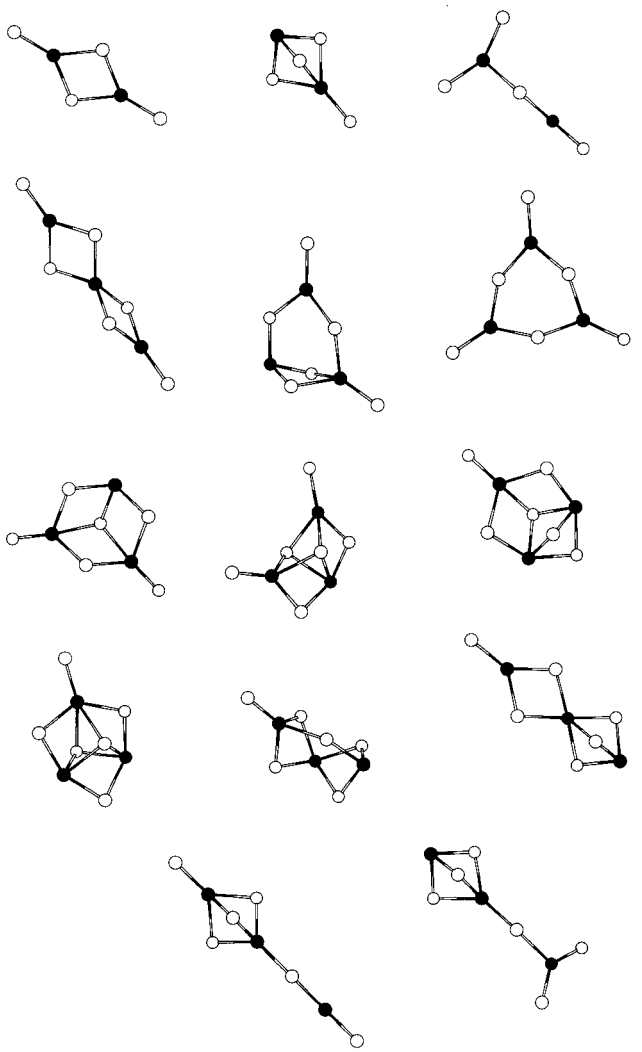

Figure 1. Inequivalent $(MgF_2)_2$ (first row) and $(MgF_2)_3$ (rows second to fourth) clusters obtained after the atomistic Monte Carlo procedure detailed in the text. Black and white balls stand for Mg^{2+} and F^- ions, respectively.

RHF and MP2 calculations have been performed using the GAMESS system of programs,[19] with standard frozen cores at the MP2 level. All RHF and MP2 harmonic frequencies were obtained at their corresponding equilibrium geometries, using analytic derivatives. Correlated wave functions were obtained by means of the Handy et al.[20] procedure with the Gaussian 98 package.[21] All of the calculations converged to ab initio true

TABLE 1: Bond Lengths (Å) and Angles (Degree) of $(MgF_2)_2$ Isomers[a]

cluster	calc.	$R(Mg_1-F_1)$	$R(Mg_1-F_2)$	$R(Mg_2-F_2)$	α	β
$(MgF_2)_2$ (D_{2h})	this work, TZV	1.767 (1.802)	1.909 (1.950)		77.68 (78.27)	
	this work, TZV(1d)	1.744 (1.769)	1.889 (1.915)		80.63 (81.34)	
	this work, TZV(1d)+	1.743 (1.769)	1.888 (1.914)		80.57 (81.16)	
	EGM[b]	1.730	1.929		75.03	
	ref 3	1.76	2.01		91	
	refs 7 and 10[c]	1.730 (1.751)	1.880 (1.905)		81.8 (83.0)	
	ref 8[d]	1.748	1.889		81.2	
	ref 9[e]	1.733 (1.775)	1.884 (1.929)		80.8 (81.6)	
$(MgF_2)_2$ (C_{3v})	this work, TZV	1.780 (1.814)	2.035 (2.088)	1.863 (1.902)	85.55 (86.39)	76.88 (76.88)
	this work, TZV(1d)	1.756 (1.781)	2.021 (2.054)	1.839 (1.866)	87.84 (88.34)	78.23 (78.56)
	this work, TZV(1d)+	1.756 (1.781)	2.020 (2.051)	1.835 (1.862)	88.12 (88.55)	78.37 (78.66)
	EGM[b]	1.746	2.085	1.866	84.68	74.14
	ref 3	1.77	2.20	1.91	95	
	refs 7 and 10[c]	1.742 (1.761)	2.009 (2.036)	1.827 (1.852)	88.6 (89.8)	

[a] Numbers in parenthesis are MP2 values. Atoms and angles are labelled according to Figure 2. [b] Values obtained in this work using the electron gas model (EGM) of Gordon and Kim (refs 14 and 15). [c] RHF and MP2 values with a 6-31G* basis set. [d] Scaled values from RHF calculations with a 6-31+G* basis set. [e] Basis set for Mg, ref 17 augmented with two (RHF) and one (MP2) *d*-type functions. Basis set for F, DZP.

TABLE 2: Bond Lengths (Å) and Angles (Degree) of $(MgF_2)_3$ Isomers[a]

dist/angle	D_2d	D_{2d}(EGM)[b]	D_{2d} (ref 8)[c]	D_{2d} (ref 10)[d]	C_s	C_s(EGM)[b]	D_{3h}	D_{3h} (EGM)[b]
$R(Mg_1-F_1)$	1.745 (1.770)	1.731	1.749	1.731	1.753 (1.777)	1.753	1.746 (1.771)	1.735
$R(Mg_1-F_2)$	1.888 (1.913)	1.924	1.888	1.879	1.967 (1.991)	2.073	1.868 (1.891)	1.905
$R(Mg_1-F_3)$					2.063 (2.121)	1.976		
$R(Mg_2-F_2)$					1.849 (1.878)	1.854		
$R(Mg_2-F_2)$	1.891 (1.915)	1.937	1.893	1.883				
$R(Mg_2-F_5)$					1.850 (1.876)	1.861		
$R(Mg_3-F_3)$					1.885 (1.913)	1.880		
$R(Mg_3-F_4)$					1.742 (1.767)	1.738		
$R(Mg_3-F_5)$					1.904 (1.931)	1.946		
α	81.07 (81.84)	75.29	81.7		86.41 (86.66)	83.23	95.41 (96.34)	92.46
β	81.26 (81.93)	75.88	81.9		80.12 (80.69)	72.90	144.59 (143.66)	147.54
γ					84.04 (84.34)	90.88		
η					79.56 (78.93)	88.38		

[a] TZV(1d) basis set. Numbers in parenthesis are MP2 values. Atoms and angles are labelled according to Figure 2. [b] Values obtained in this work using the Electron Gas Model (EGM) of Gordon and Kim (Refs. GK72 and FR95a). [c] RHF calculations with a 6-31+G* basis set. [d] RHF calculation using a 6-31G* basis set.

local minima with final geometries clearly related and actually very similar to the starting configurations.

III. Structural and Energetic Properties

A. Geometry. We present in Tables 1 and 2 the optimized geometries of the selected $(MgF_2)_n$ ($n = 2-3$) isomers. The optimum atomistic geometries used as starting points for the ab initio minimizations are also included for comparison purposes.

General basis set and correlation effects follow closely our conclusions for the monomer. The Mg−F distances are shortened by 0.020−0.040 Å when a *d* polarization function is included in the calculation and do not change appreciably with the use of diffuse *s* and *p* functions. At the TZV(1d) level, all of the R(Mg−F) interatomic distances, except $R(Mg_1-F_2)$ in $(MgF_2)_2$ (C_{3v}) and $R(Mg_1-F_3)$ in $(MgF_2)_3$(C_s), increase by 0.023−0.028 Å on going from the RHF to the MP2 correlated picture. On the contrary, F−Mg−F bonding angles turn out to be fairly insensitive to correlation corrections. Geometrical effects of the MP2 correlation may be thus viewed as a breathing expansion of the RHF clusters, with distances enlarged by a 1.2−1.4% factor. The role of polarization on distances is contrary in sign while similar in magnitude to that of correlation. This is the rationale behind the good RHF results with unpolarized basis sets.

A more detailed analysis of our results shows very interesting correlations. One of the easiest to observe is the clear variation of the Mg−F distances with the classical coordination indices of both the cation and the anion. Terminal fluorides are bonded to tri- or tetracoordinated Mg atoms. At the MP2/TZV(1d) level, their bonded distances are 1.769 ± 0.002 Å and 1.779 ± 0.002 Å, respectively. These remarkably constant distances are to be compared with their equivalent values in the monomer (1.769 Å) and the pure diatomic MgF (1.759 Å). This behavior is well-known in ionic clusters, and results from the anion−anion additional Coulombic repulsions that arise as the number of anions bonded to one cation grows. A similar analysis for the nonterminal F−Mg distances clearly reveals that they increase with coordination. The largest value at the MP2/TZV(1d) level, 2.121 Å, is found in the C_s trimer for the Mg_1-F_3 pair, with a four-coordinated magnesium and a (3 + 3)-coordinated fluoride. An illuminating plot of these relationships, as well as of the effects of correlation corrections on the distances, is found in Figure 3.

Anion−anion distances are usually not considered in these kinds of studies. This is mainly due to the difficulty in choosing appropriately related anion pairs. The AIM theory provides a well-founded and unique route to face the problem. Only bonded anionic pairs should be directly compared. Doing so, distances between bonded fluorides turn out to be rather constant, 2.496−2.600 Å and to increase with the AIM coordination, in the same way as other interionic distances do.

It is interesting to notice that the differences between Mg-terminal-F and Mg-nonterminal-F, as well as the overall geometrical features of the clusters, are fairly well reproduced by both Gigli[3] and our EGM results. A deeper analysis of this

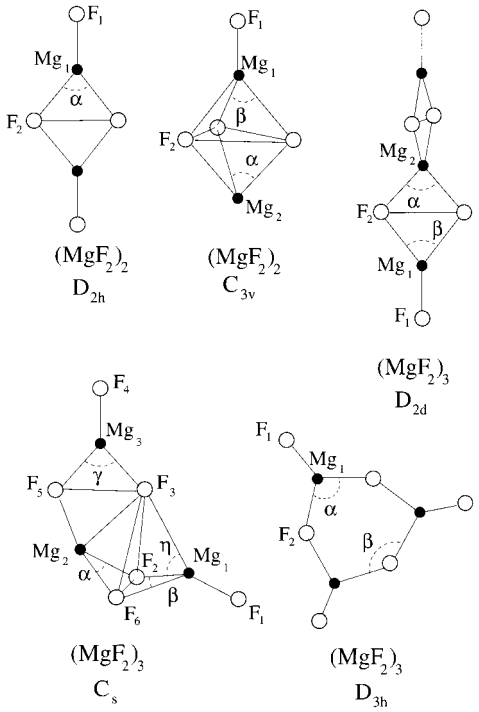

Figure 2. $(MgF_2)_n$ ($n = 2-3$) clusters investigated by ab initio procedures in this work. Solid lines connecting a pair of atoms define the molecular graph as determined in section IV using the atoms in molecules theory.

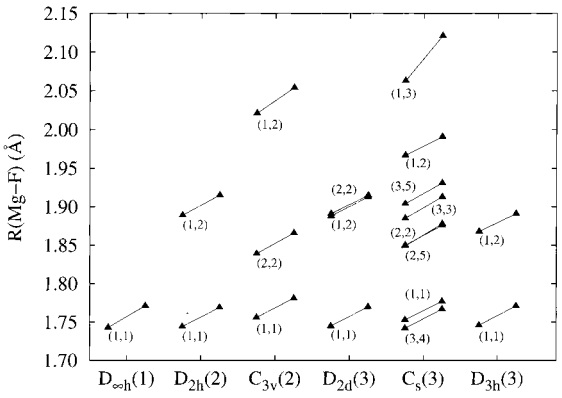

Figure 3. Mg−F equilibrium distances of the bonded (Mg,F) pairs. Each of these pairs is indicated according to the labels in Figure 2. The left and right points shown in each line stand for the RHF and MP2 values, respectively. The number in parentheses in the abscissa labels refers to the n value of the isomer $(MgF_2)_n$.

success in terms of the AIM results and the resulting PIM model will be presented below.

B. Energetic Properties. Total energies for the selected dimers and trimers are given in Table 3. Inclusion of *d* polarization functions (from TZV to TZV(1d)) decreases the total energy per MgF_2 unit by 0.6−0.7 eV in the RHF calculations and by a number as large as 4−5 eV in the MP2 results. This shows the important role of the *d*-type functions on computing the correlation energy. As shown in paper I, this is mainly a geometrical effect that is due to the strong dependence of the correlation correction on interatomic distances. The addition of a set of diffuse *s* and *p* functions (TZV(1d)+ basis set) decreases the TZV(1d) energies by less than 0.1 eV.

In the dimer, these results agree qualitatively with those of Ramondo et al.[7] and Axten et al.,[10] because we clearly predict the D_{2h} isomer to be some 0.7 eV below the C_{3v} structure. This

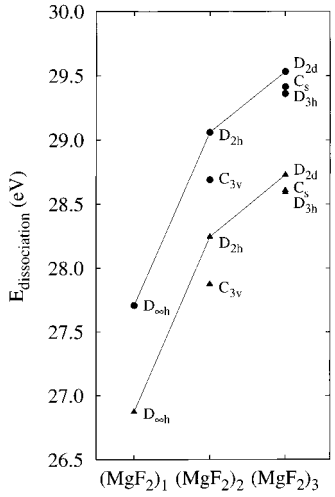

Figure 4. Dissociation energy per MgF_2 unit. The two solid lines connect the less energetic isomers of the monomer, dimer, and trimer, i.e., $D_{\infty h}$ ($n = 1$), D_{2h} ($n = 2$), and D_{2d} ($n = 3$). HF/TZV(1d) and MP2/TZV(1d) dissociation energies are represented by triangles and circles, respectively.

number is, however, 0.1−0.2 eV greater than the value reported in refs 7 and 10. As usual, when considering isoelectronic compounds, the correlation corrections depend very slightly on the nuclear geometries, and their effects upon the relative stability of both isomers is smaller than 0.03 eV in all of the cases. As the trimer is concerned, the most stable isomer is found to be the double-bridged D_{2d} structure. This is followed by the C_s form at 0.366/0.356 eV and by the D_{3h} structure at 0.413/0.518 eV above the D_{2d} isomer. The pairs of numbers refer to the RHF/MP2 descriptions with the TZV(1d) basis set, respectively. The trimer is, therefore, the first $(MgF_2)_n$ cluster in which the most stable structure is nonplanar. This tendency is also well-known and is due to the dependence of dipole−dipole stabilizing interactions with the dipoles' parallelism. In fact, Table 3 shows that the EGM model predicts the D_{3h} planar isomer as the most stable one. We will investigate this issue further in Section V.

Some experimentally accessible energetic magnitudes deserve consideration. The dissociation energy per MgF_2 unit, (DE), defined as the energy of the reaction $1n(MgF_2)_n \rightarrow Mg^{2+} + 2F^-$, is represented in Figure 4. As it can be seen, the stability against decomposition into Mg^{2+} and F^- ions increases steadily with the cluster size, independently of the isomer considered and of whether correlation effects are included or not. This behavior is the expected one. Much more interesting is the growing rate of this magnitude with size coordinates. The rutile bulk limit value, $DE(n \rightarrow \infty) = 30.64$ eV,[22] is roughly 4 eV above the monomer's experimental value (see paper I). This difference is already halved for the trimer. This fast convergence of molar binding energies is typical of ionic compounds. Table 4 contains our ab initio and EGM DE values together with the results reported by Gigli[3] and the available experimental data. The lack of dipole−dipole interactions in the EGM calculations generates too low DE values, about 1−2 eV below the ab initio results. Both Gigli's results and our polarizable-ions model (see Table 11) improve these values considerably. Following closely the findings of paper I, the dimer's RHF DE agrees fairly well with the experimental value, whereas correlated figures worsen this agreement. We also find here that the addition of polarization functions changes the sign of the MP2 corrections to the DEs.

We have also computed the fragmentation energies (FEs) of $(MgF_2)_2$ and $(MgF_2)_3$ clusters for several fragmentation channels.

TABLE 3: Total Energy (hartree) of $(MgF_2)_n$

molecule	basis set	RHF	MP2
$(MgF_2)_2$ (D_{2h})	TZV	−797.443 816	−798.063 718
	TZV(1d)	−797.492 774	−798.401 490
	TZV(1d)+	−797.496 330	−798.410 849
	ref 10[a]	−797.316 785	−798.109 871
$(MgF_2)_2$ (C_{3v})	TZV	−797.418 052 (0.701)[b]	−798.037 054 (0.726)[b]
	TZV(1d)	−797.465 542 (0.741)[b]	−798.374 370 (0.738)[b]
	TZV(1d)+	−797.469 699 (0.725)[b]	−798.384 433 (0.719)[b]
	ref 10[a]	−797.291 599 (0.685)[b]	−798.088 389 (0.585)[b]
$(MgF_2)_3$ (D_{2d})	TZV(1d)	−1196.292 334	−1197.654 481
	ref 10[a]	−1196.033 670	
$(MgF_2)_3$ (C_s)	TZV(1d)	−1196.278 877 (0.366)[c]	−1197.641 395 (0.356)[c]
$(MgF_2)_3$ (D_{3h})	TZV(1d)	−1196.277 171 (0.413)[c]	−1197.635 461 (0.518)[c]

[a] Calculation with a 6-31G* basis set. MP2 calculations with all the orbitals active. [b] Energy (eV) above the D_{2h} configuration. [c] Energy (eV) above the D_{2d} configuration.

TABLE 4: Dissociation Energy ($(MgF_2)_n \rightarrow n Mg^+ + 2n F^-$) (eV) Per MgF_2 Unit

molecule	basis set	RHF	MP2
$(MgF_2)_2(D_2h)$	TZV	27.579	24.463
	TZV(1d)	28.245	29.059
	TZV(1d)+	28.294	29.186
	EGM[a]	26.210	
	ref GI90	27.04	
	expt (ref 23)	27.75	
$(MgF_2)_2$ (C_{3v})	TZV	27.229	24.100
	TZV(1d)	27.875	28.690
	TZV(1d)+	27.932	28.827
	EGM[a]	25.697	
	ref 3	26.63	
$(MgF_2)_3$ (D_{2d})	TZV(1d)	28.728	29.532
	EGM[a]	26.683	
$(MgF_2)_3$ (C_s)	TZV(1d)	28.606	29.414
	EGM[a]	26.682	
$(MgF_2)_3$ (D_{3h})	TZV(1d)	28.590	29.360
	EGM[a]	26.732	
Rutile, expt[b]		30.64	

[a] Values obtained in this work using the electron gas model (EGM) of Gordon and Kim (refs 14 and 15). [b] Reference 22.

Results are shown in Table 5. As expected, our best MP2/TZV(1d) numbers are just 0.05−0.20 eV smaller than the RHF/TZV(1d) values, showing the roughly additive character of correlation corrections in these systems. The FE of the D_{2h} isomer of $(MgF_2)_2$, 2.747 and 2.702 eV at the RHF/TZV(1d) and MP2/TZV(1d) levels, respectively, agrees very well with minus the estimated experimental value for the heat of dimerization of MgF_2 at 298 K, which is 2.749 eV.[22] Our FEs for both the D_{2h} and C_{3v} dimers are ∼0.3 eV smaller than the values reported by Axten et al.[10] in their RHF/6-31G* calculations. When correlation energy corrections at the MP2 level are included, the FEs given by Axten et al. are ∼0.5 eV greater than ours. Moreover, these authors obtain MP2 FEs greater than their RHF numbers, a result which is contrary to the findings of this work.

Clusters are often produced and studied in highly energetic jets. Though nonequilibrium phenomena are very important in these conditions and thermodynamical arguments must be applied with care, temperatures reach very high values in the jets. This fact may have important consequences in the actual clusters that are found experimentally. According to our results, dimers and trimers should be found in their D_{2h} and D_{2d} forms at zero temperature (neglecting zero-point vibrational effects). At finite T, however, the equilibrium populations of different isomers are determined by the Helmholtz free energy, $A = -kT \ln Q$, where Q is the canonical partition function.[24] It follows that for a specific $(MgF_2)_n$ cluster, the relative population of the ith isomer is given by $C_i = Q_i/\sum_i Q_i$, with i running over all of the isomers of this cluster. From the total energies and harmonic vibrational frequencies (see below), we have computed the C_i values for $(MgF_2)_2$ and $(MgF_2)_3$. The results are presented in Figure 5, where the approximation that higher energy isomers (not investigated in this work) do not contribute to the above denominator has been made. We find that for $T < 2000$ K, the D_{2h} isomer of the dimer is the only one having a significant population. For greater temperatures, the concentration of the C_{3v} isomer increases almost linearly with T, reaching ≃10% at $T = 10^4$ K. As the trimer is concerned, the concentration of the D_{2d} isomer (the energetically most stable one) progressively decreases from 100% at 0 K down to ≃22% at $T = 10^4$. On the contrary, the concentration of the D_{3h} isomer increases from 0% at 0 K up to ≃64% at 10^4 K, with a crossing point with the D_{2d} at about $T = 3600$ K. Interestingly, the C_s isomer, more stable at 0 K than the D_{3h} structure, reaches a constant concentration of 4% at about 3500 K. These conclusions apply to thermodynamic equilibrium conditions. If the formation of dimers and trimers is kinetically controlled, the actual populations of the different isomers should be discussed in terms of the conversion rate of the reactions $D_{2h} \rightleftharpoons C_{3v}$ for $(MgF_2)_2$ and $D_{2h} \rightleftharpoons D_{3h} \rightleftharpoons C_s$ for $(MgF_2)_3$. This kinetic study is beyond the objectives of this paper.

C. Harmonic Vibrational Frequencies. Experimental IR and Raman vibrational bands of $(MgF_2)_n$ and their assignments according to different authors[2,25−27] are collected in Table 6. Our theoretical frequencies for $(MgF_2)_2$ ($n = 2-3$) appear in

TABLE 5: Fragmentation Energies (eV) of $(MgF_2)_n$ Clusters

reaction			this work[a]	ref 7[b]	ref 10[c]
$(MgF_2)_2(D_2h)$	→	2 MgF_2 ($D_{\infty h}$)	2.747 (2.702)	(3.161)	3.045 (3.162)
$(MgF_2)_2(C_3v)$	→	2 MgF_2 ($D_{\infty h}$)	2.006 (1.964)	(2.581)	2.359 (2.576)
$(MgF_2)_3(D_2d)$	→	$(MgF_2)_2$ (D_{2h}) + MgF_2 (D $_{\infty h}$)	2.820 (2.772)		
$(MgF_2)_3(C_s)$	→	$(MgF_2)_2$ (D_{2h}) + MgF_2 (D $_{\infty h}$)	2.454 (2.416)		
$(MgF_2)_3(D_3h)$	→	$(MgF_2)_2$ (D_{2h}) + MgF_2 (D $_{\infty h}$)	2.408 (2.255)		
$(MgF_2)_3(D_2d)$	→	3MgF_2 ($D_{\infty h}$)	5.567 (5.474)		6.163
$(MgF_2)_3(C_s)$	→	3MgF_2 (D$_{\infty h}$)	5.201 (5.118)		
$(MgF_2)_3(D_3h)$	→	3MgF_2 ($D_{\infty h}$)	5.154 (4.957)		

[a] Results with the TZV(1d) basis set. Numbers in parentheses are MP2 values. [b] Calculations using 6-31G* basis set. [c] Calculations using a 6-31G* basis set.

TABLE 6: Experimental Infrared (Except where Indicated) Vibrational Frequencies (cm^{-1}) of $(MgF_2)_n$ and Their Assignments

frequency	Snelson[a]	Mann et al.[b]	Hauge et al.[c]	Lesiecki and Nibler[d]
240[b,d]		MgF_2, $(MgF_2)_n$		$(MgF_2)_2$
248,[a] 249.0[d]	MgF_2			MgF_2
354 (Raman)[d]				$(MgF_2)_2$
450[b,d]		$(MgF_2)_n$		$(MgF_2)_2$
477[b]		MgF_2		
490,[a] 483,[b] 486.6,[c] 486.5[d]	$(MgF_2)_n$	$(MgF_2)_n$	$(MgF_2)_2$	$(MgF_2)_2$
548.0[d]				MgF_2...X (?)
550.0 (Raman)[d]				MgF_2
584 (Raman)[d]				$(MgF_2)_2$
(738.2, 732.8, 726.5)[b]		MgF		MgF(?)
745,[a] 746.5,[c] (745.9, 741.1, 735.4)[d]	$(MgF_2)_n$		$(MgF_2)_2$	$(MgF_2)_2$
850,[a] 840,[b] 842.3,[c] 841.8[d]	MgF_2	MgF_2	MgF_2	MgF_2

[a] Reference 25. [b] Reference 26. [c] Reference 27. [d] Reference 2.

TABLE 7: Vibrational Frequencies (cm^{-1}) of $(MgF_2)_2$

freq.	TZV(1d)[a]	TZV(1d)+[a]	ref 7[b]	ref 9[c]	ref 10[d]	ref 8[e]	expt[f]
			D_2h Isomer				
B_{2g}	142.6 (141.9)[g]	139.1 (138.0)	159 [132]	128 (130)	131.7	123	
B_{1g}	150.6 (147.8)	150.5 (147.1)	185 [158]	157 (154)	158.3	146	
A_g	270.2 (259.3)	269.6 (259.1)	290 [276]	271 (258)	276.0	253	353
B_{1g}	460.0 (447.2)	455.9 (442.4)	516 [469]	453 (440)	468.9	431	
A_g	512.5 (482.8)	512.7 (482.8)	549 [523]	517 (475)	523.2	481	585
A_g	834.2 (800.7)	832.8 (796.6)	947 [864]	844 (782)	863.6	775	
B_{1u}	59.0 (57.0)	57.98 (56.17)	63 [54]	54 (52)	53.8	52	
B_{2u}	103.5 (101.1)	104.8 (102.3)	123 [109]	107 (105)	109.5	100	
B_{1u}	286.1 (272.7)	287.8 (276.6)	297 [284]	284 (268)	284.4	266	240
B_{3u}	479.5 (457.4)	479.2 (456.5)	525 [490]	480 (453)	490.2	450	450
B_{2u}	507.8 (491.1)	507.0 (488.5)	563 [534]	515 (484)	534.6	484	487
B_{3u}	809.9 (778.2)	808.2 (774.1)	920 [838]	818 (746)	837.9	752	747
			C_{3v} Isomer				
E^h	132.0 (126.1)		154 [133]		133.4		
E^h	269.9 (255.9)		323 [282]		281.9		
E^h	309.9 (289.6)		337 [312]		312.0		
$A_1{}^h$	339.7 (325.6)		369 [353]		353.1		
$A_1{}^h$	420.3 (395.1)		451 [432]		431.6		
E^h	590.6 (564.6)		648 [614]		613.6		
$A_1{}^h$	639.7 (606.1)		688 [657]		656.6		
$A_1{}^h$	787.1 (757.8)		901 [819]		819.3		

[a] This work. [b] Calculations using a 6-31G* basis set. Numbers in brackets [] are RHF results in the MP2 optimized geometry. [c] Basis set for Mg, ref MC80 augmented with two (RHF) and one (MP2) *d*-type functions. Basis set for F, DZP. [d] RHF calculation using a 6-31G* basis set. [e] Scaled values from RHF calculations with a 6-31+G* basis set. [f] $(MgF_2)_2$ in argon matrix. Assignment of M. L. Lesiecki and J. W. Nibler, ref 2. [g] Numbers in parentheses are MP2 results. [h] The ν_i values of this isomer are simply ordered by increasing energy and not according to their classification as Raman or infrared active bands of the D_{2h} isomer.

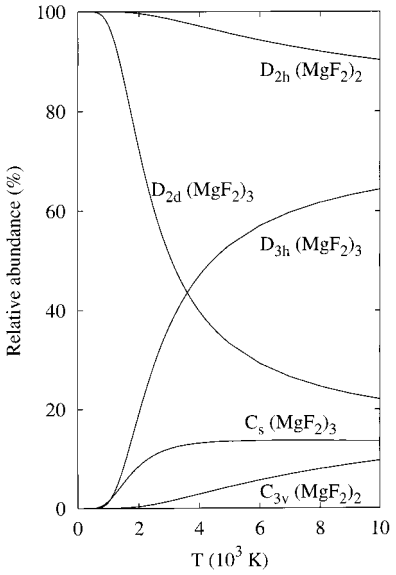

Figure 5. Relative abundance of the D_{2h} and C_{3v} isomers of $(MgF_2)_2$ and of the D_{2d}, C_s, and D_{3h} isomers of $(MgF_2)_3$ as a function of temperature.

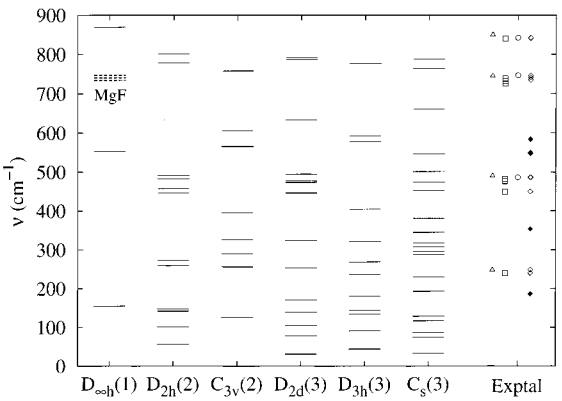

Figure 6. Theoretical (MP2/TZV(1d)) and experimental frequencies of the most stable isomers of $(MgF_2)_n$ ($n = 1-3$). The experimental results of Snelson,[24] Mann et al.,[25] Hauge et al.,[26] and Lesiecki and Nibler[1] are represented by triangles, squares, circles, and diamonds, respectively. Empty and filled symbols stand for infrared and Raman spectra, respectively.

Tables 7 ($n = 2$) and 8 ($n = 3$). To make easier the comparison, we have plotted in Figure 6 the computed MP2/TZV(1d) frequencies and the experimental results. The MP2/TZV(1d)+ frequencies of the monomer and of the ^{24}MgF, ^{25}MgF, and ^{26}MgF diatomic molecules have been also plotted in Figure 6.

Relatively firm conclusions may be made about the assignment made by Mann et al. (M)[26] and Lesiecki and Nibler (LN)[2]

TABLE 8: Vibrational Frequencies (cm^{-1}) of $(MgF_2)_3$

frequency	D_{2d}[a]	ref 10[b]	ref 8[c]	D_{3h}[a]	C_s[a]
ν_1(E)[d]	30.8	31.3	33	43.7	34.0
ν_2(E)	31.8	31.3	33	45.9	74.3
ν_3(B_1)	78.5	78.2	77	45.9	87.3
ν_4(E)	104.4	99.3	98	90.8	116.9
ν_5(E)	104.9	99.3	98	90.8	128.5
ν_6(E)	139.3	139.0	135	134.4	128.9
ν_7(E)	139.7	139.0	135	144.3	192.9
ν_8(A_1)	170.5	182.8	168	144.3	230.9
ν_9(E)	253.3	264.1	247	180.6	287.8
ν_{10}(E)	253.5	264.1	247	180.6	296.5
ν_{11}(B_2)	324.6	343.3	317	236.4	307.7
ν_{12}(A_1)	444.5	473.6	437	269.0	317.5
ν_{13}(E)	448.3	468.8	432	320.6	345.1
ν_{14}(E)	448.5	468.8	432	404.4	381.1
ν_{15}(B_2)	473.7	509.5	469	404.4	452.6
ν_{16}(A_1)	477.0	514.9	474	577.2	474.6
ν_{17}(E)	494.7	538.5	488	577.2	501.5
ν_{18}(E)	494.9	538.5	488	591.7	546.4
ν_{19}(B_2)	633.1	665.5	609	776.4	661.7
ν_{20}(B_2)	786.2	846.1	760	776.4	763.5
ν_{21}(A_1)	791.5	850.7	765	776.9	787.9

[a] MP2 results of this work with a TZV(1d) basis set. [b] RHF calculation using a 6-31G* basis set. [c] Scaled values (scale factor 0.94) from RHF calculations with a 6-31+G* basis set. [d] Symmetry labels are only valid for the D_{2d} isomer.

of an experimental band about 240 cm^{-1} to polymeric and dimeric MgF_2, respectively. This assertion is well supported by our data, as we predict two bands for the dimer and one band for the trimer at a frequency slightly higher than 250 cm^{-1}. The Raman band observed by LN at 186 cm^{-1} in solid argon, and tentatively assigned by these authors to a nonfluorinated species, occurs at higher frequencies than those computed for our dimer and trimer soft modes. However, the strong dependency of this band on the environment[2] does not preclude it to be assigned to $(MgF_2)_2$ and/or $(MgF_2)_3$. Concerning the Raman band at 354 cm^{-1}, LN suggest that it might be due to the A_g Raman-active vibration mode of D_{2h} $(MgF_2)_2$. Our prediction at 270 cm^{-1} is 84 cm^{-1} below the alleged observed value. In our opinion, this discrepancy is too high to be due to theoretical shortcomings. On the contrary, we believe that it can be assigned to the ν_7 or ν_8 band of C_{3v} $(MgF_2)_2$. At the MP2/TZV(1d) level, these bands appear at 325.58 and 395.10 cm^{-1}, respectively. In the same way, a feature near 585 cm^{-1} that only appears in concentrated matrixes is assigned by LN to another A_g Raman active mode of D_{2h} $(MgF_2)_2$. As our MP2/TZV(1d) prediction for this band is 482.78 cm^{-1}, we suggest that the feature at 585 cm^{-1} can be attributed to the ν_9 (E), ν_{10} (A_1), or ν_{11} (E) vibration modes of C_{3v} $(MgF_2)_2$.

An IR-active band calculated at 457.35 cm^{-1} in the dimer and two degenerate IR-active frequencies computed at 448 cm^{-1} in the trimer support the assignment of M[26] and LN[2] of the observed IR-active band at 450 cm^{-1} to $(MgF_2)_2$ or $(MgF_2)_3$. The IR spectra of refs 2 and 25−27 also detect a band at about 480−490 cm^{-1}, invariably assigned to $(MgF_2)_2$ or $(MgF_2)_3$. The theoretical results displayed in Figure 5 completely support this assignment, because a set of six frequencies coming from $(MgF_2)_2$ and $(MgF_2)_3$ are predicted in the interval 470−500 cm^{-1}. Also in agreement with LN, we think that the IR band observed by M at 477 cm^{-1} cannot be ascribed to MgF_2 or a polymeric species.

Finally, M also reports a triplet at (738.2, 732.8, 726.5) $cm^{-1}$and assigns it to (^{26}MgF, ^{26}MgF, ^{26}MgF). A similar triplet is observed by LN at (745.9, 741.1, 735.4), this time associated to $(MgF_2)_2$ without completely discarding the suggestion of M. None of our theoretical frequencies for the dimer or the trimer are close to these values. On the contrary, our MP2/TZV(1d)+ prediction for the isotopic MgF triplet is (746.75, 740,11, 733,-95) cm^{-1}, with these results making it likely that this triplet might be due to the reduced species MgF.

IV. Bonding in Light of the AIM Theory

The usefulness of the AIM theory to rationalize and physically interpret the results of quantum chemical calculations in this kind of system has already been shown. We refer the reader to section IV of paper I for such an account. Suffice it to say that the monomer turns out to be a highly ionic molecule, with almost nominal atomic charges and nonnegligible atomic polarizabilities. This image induces a polarizable-ions model that accounts fairly well for the observed molecular properties.

Our present dimers and trimers expand a richer variety of bonding possibilities than that expected in the monomer. As shown in paper I, only large polarized basis sets are able to saturate the atomic multipoles in AIM analyses. Therefore, we will only discuss our RHF or MP2 TZV(1d) results. The plain topology of the ρ scalar field gives rise to the chemical graphs depicted in Figure 2. Each solid line represents a bond path. All neighboring Mg−F pairs are connected by a bond path, as expected. Selected anionic pairs are also bonded. Notice that Mg atoms are never bonded among themselves. This is the usual behavior found in ionic systems, and it is traced back to their compact electron densities. It is also relevant to point out that the D_{3h} trimer lacks F−F bonds and that it is this isomer the one with largest Mg−F−Mg angles (96.34° at the MP2 level). We feel that this is a clear manifestation of the role that anion−anion bond paths may play in these systems. A ring critical point (CP) has been found at about the center of each ring of bond paths. Two sets of two cage CPs have also been found in the C_{3v} dimer and the C_s trimer. The topology of all of the clusters is therefore of the normal kind.

Densities and Laplacians at Mg−F bond CPs do not show significant deviations from those found for the monomer in paper I, so our discussion here will be very succinct. The variation found in their values at a given computational level just reveals the slightly different set of bond distances of our clusters. It is once again found that the logarithms of densities and Laplacians are perfectly proportional to the bond distances, as the tail model of the ionic densities dictates. All of the Mg−F bonds found are just slightly different flavors of the same chemically distinctive ionic interaction. The new F−F interactions do not contain significantly new information, with it being characterized by very small densities and positive Laplacians at the bond CPs.

Much more interesting is the study of the AIM electronic multipoles and their variation with bond distances and coordination indices. Table 9 collects the RHF and MP2 TZV(1d) charge monopoles, or atomic charges, found for our clusters. The monomer and rutile values are also included for completeness. The net charges of the cations gather around $+1.8|e|$ and those of the fluorides around $-0.9|e|$. These are almost nominal charges, practically identical to those found in the monomer. This fact, together with the absence of a valence shell in the cationic Laplacian fields, points toward a mostly electrostatic picture. A finer-grained analysis of the data gives a convincing proof of the ability of these quantities to capture the details of the interactions. The charges of terminal fluorides lie in the range of $-0.915 \pm 0.004|e|$/ $-0.894 \pm 0.005|e|$ at the RHF/MP2 levels, respectively, whereas the analogue figures for the bridging anions are $-0.919 \pm 0.009|e|$/ $-0.907 \pm 0.010|e|$. It is clear that these charges increase (in absolute value) with the

TABLE 9: AIM Topological Charges of $(MgF_2)_n$ (n =1−3) Obtained with the TZV(1d) Basis Set at the Theoretical RHF (First Row) and MP2 (Second Row) Equilibrium Geometries

molecule	Mg_1	Mg_2	Mg_3	F_1	F_2	F_3	F_4	F_5
MgF_2 ($D_{\infty h}$)	1.826			−0.913				
	1.786			−0.893				
$(MgF_2)_2$ (D_2h)	1.825			−0.912	−0.913			
	1.791			−0.891	−0.900			
$(MgF_2)_2$ (C_{3v})	1.826	1.838		−0.918	−0.915			
	1.794	1.805		−0.899	−0.900			
$(MgF_2)_3$ (D_2d)	1.825	1.828		−0.912	−0.913			
	1.790	1.798		−0.892	−0.899			
$(MgF_2)_3$ (D_3h)	1.827			−0.913	−0.916			
	1.795			−0.892	−0.904			
$(MgF_2)_3$ (C_s)	1.827	1.833	1.829	−0.916	−0.913	−0.927	−0.911	−0.910
	1.795	1.802	1.796	−0.897	−0.897	−0.916	−0.889	−0.895
rutile[a]	1.889			−0.944				

[a] Reference 12.

TABLE 10: Atomic Electron Dipoles (First Row) and Quadrupoles (Second Row) for $(MgF_2)_n$ (n = 1−3) Obtained at the TZV(1d)/MP2 Level[a]

molecule	Mg_1	Mg_2	Mg_3	F_1	F_2	F_3	F_4	F_5
MgF_2 ($D_{\infty h}$)	0.000			0.293				
	0.39			0.78				
$(MgF_2)_2$ (D_2h)	0.010			0.271	0.141			
	0.26			0.79	0.76			
$(MgF_2)_2$ (C_{3v})	0.004	0.016		0.245	0.148			
	0.20	5.6×10^{-3}		0.899	0.900			
$(MgF_2)_3$ (D_2d)	1.825	1.828		0.912	0.913			
	1.790	1.798		0.892	0.899			
$(MgF_2)_3$ (D_3h)	1.827			0.913	0.916			
	1.795			0.892	0.904			
$(MgF_2)_3$ (C_s)	1.827	1.833	1.829	0.916	0.913	0.927	0.911	0.910
	1.795	1.802	1.796	0.897	0.897	0.916	0.889	0.895

[a] Only the modulus of the dipole and the leading eigenvalue of the traceless quadrupolar tensor are shown. Atomic units are used throughout.

coordination index, as chemical intuition indicates, and that electron correlation tends to enhance the effect. If we take a closer look at the terminal fluorides, a neat proportionality among charge and bond distance emerges. This fact is to be rationalized in terms of the Pauling−Brown rules, which establish an empirical relationship among coordination indices and bond distances. Cationic charges follow equivalent trends.

Dipolar and quadrupolar moments integrated in the atomic basins are shown in Table 10. Overall, there are no significant differences with respect to the monomer. The trends shown by the fluorides' dipoles run parallel to those of the monopoles. All fluorides are forward polarized toward the nearest magnesiums, showing their labile valence electronic distributions. Terminal fluorides classify themselves according to the coordination index of the neighboring magnesium. There is a clear decrease in the absolute valence density distortion of the F^- ion on going from two- to four-coordinated Mg^{2+}. This is basically due to the electrostatic effect of the second neighbor fluorides, as we will see below. Bridging fluorides display smaller dipoles, as their more symmetrical environments suggest, and correlate also with coordination. Magnesiums show very small dipolar moments because of both the low polarizability of their cores (see paper I) and their more symmetric positions. In all cases, every bonded fluoride counter-polarizes the Mg^{2+} core, and the final direction of the dipole is that of the winner set of fluorides. In this way, we understand, for example, why the density of Mg_1 in the C_{3v} isomer is displaced toward the terminal F_1, giving a dipole moment around 4×10^{-3} a.u., whereas the density of Mg_2 moves toward the equatorial plane, with a final dipole almost four times larger. Using these ideas, the trends found are easily rationalized. Notice the very small dipole moments of the bridging fluorides in the D_{3h} isomer.

As quadrupoles are concerned, and given the different environments found in the clusters, we will concentrate on the leading eigenvalue (Q) of the traceless quadrupolar atomic tensor. The magnitude of this property shows the same type of correlations with distance, coordination, or net charge that we have been discussing. As found in the monomer, the atomic distributions are always slightly oblate or compressed. Terminal fluorides display Q values almost indistinguishable from those in the monomer, whereas bridge fluorides show somewhat smaller values, approaching sphericity. Magnesiums are slightly less distorted here than in the monomer, and particularly small values of Q are found in the cations that are not bonded to a terminal fluoride. This illustrates that the cationic density

compressions are very dependent on distance and that terminal fluorides determine it.

V. Discussion and Modeling

The tools of the AIM theory were shown in paper I to provide the basis for a polarizable-ions model that accounts fairly well for the physical properties of the MgF_2 monomer. The greater number of systems of the present work allow us to face this strategy with more generality, as now we may use the bonding network as a new taxonomic criterion.

For example, one of the more relevant questions on clusters, as intermediates between gas phase and condensed matter, is the characterization of the building blocks involved in nucleation and crystal growth processes. The ab initio study of how the bulklike properties emerge from clusters of increasing sizes is prohibitive in computer time, but very interesting conclusions can be derived from the analysis of the bonding networks of clusters as small as $(MgF_2)_2$ and $(MgF_2)_3$. First of all, we observe that the $D_{2d}(MgF_2)_3$ is made of two $D_{2d}(MgF_2)_2$ that share a Mg atom and have lost a F atom each. Distances and angles hardly change in this process. More interesting is the discussion concerning the C_s isomer, as it was only after the molecular graphs for all of the structures were established that it became crystal clear that the C_s structure can be obtained from the C_{3v} and D_{2h} isomers of $(MgF_2)_2$. A detailed comparison between the distances and angles of the $D_{2h}$and C_s isomers actually shows that the subsets $Mg_1(F_1F_2F_2)$ (D_{2h}) and $Mg_3(F_4F_3F_5)$ (C_s) are geometrically almost equivalent. Similarly, the sets $Mg_2(F_2F_3F_6)$ Mg_1F_1 (C_s) and $Mg_2(F_2F_2F_2)$ Mg_1F_1 (C_{3v}) present corresponding equilibrium distances and angles very similar to each other.

The results are not conclusive, and additional work should be done along these lines. We must stress, however, that an EGM study on $(MgF_2)_n$ ($n \geq 3$) clusters[28] seems to indicate that most of the stable structures found can be built from four basic building blocks, namely, (1) a planar or quasiplanar Mg_2F_2 rhombus, (2) a trigonal bipyramidal MgF_3Mg, (3) a planar or quasiplanar MgF_3 unit with a tricoordinated Mg atom, and (4) a tetrahedral MgF_4 unit with a tetracoordinated Mg atom.

Concerning the PIM model, we have used the previously presented EGM short-range potentials supplemented with topological point charges and atomic electric dipoles generated by the constant polarizabilities used in paper I ($\xi = 0.7$ and 2.3 au for Mg^{2+} and F^-, respectively). The geometry optimizations improve considerably the bare EGM results. The use of topological charges uniformly increases all distances, and the nonzero polarizabilities decrease the size of the clusters and open the low F−Mg−F EGM angles. The nonzero polarizability of the cations is important in determining good F−Mg−F angles. To simplify the discussion as much as possible, we will only show in detail the results for the D_{2h} isomer. Optimized geometrical parameters turn out to be as follows: $R(Mg_1-F_1) = 1.712$ Å, $R(Mg_1-F_2) = 1.95$ Å, $\alpha = 81.8°$. These are to be compared with the results of Table 1. The vibrational spectrum is also very well predicted, and harmonic frequencies in the same order as in Table 7 are 126, 148, 238, 302, 476, 754, 52, 104, 261, 409, 501, and 754 cm^{-1}. Final dipole moments are also in rather good agreement with the ab initio results.

The PIM is key to understand the relative energetic ordering of the isomers of a given stoichiometry, this question being homologous to the bending problem posed in paper I. The energetic order of the three $(MgF_2)_3$ clusters (D_{2d}, C_s, D_{3h}) is not matched by a rigid pair potential simulation but actually reversed (D_{3h}, C_s, D_{2d}). This result remains unchanged if nominal charges are varied. Interestingly enough, almost any PIM simulation restores the ab initio ordering. Table 11 gathers the total binding energy of the clusters under the PIM, with and without polarization corrections, together with a partition of the polarization energy into atomic contributions. Despite the fact that cationic polarizability is relevant to our discussion, the final polarization energy of the Mg atoms is very small and has not been included. It is clearly seen that all of the terminal fluorides feel an almost identical electric field. Concerning the bridging anions, all of them are rather similar in all of the isomers but the D_{3h} one. The electric field at the bridge fluorides is very small in this case because of the planar molecular configuration. This is an effect found many times in the atomistic simulation of clusters, and it is usually stated that polarization corrections favor nonplanar molecules against planar ones. This explains why the stabilization achieved by including polarization corrections in the D_{2d} and the C_s molecules is practically identical and much higher than in the D_{3h} isomer. This is sufficient to reverse the rigid potential ordering of the isomers, and rationalizes the low ab initio dipole moment previously found for the bridging fluorides of the D_{3h} cluster.

TABLE 11: PIM Total Binding Energies of $(MgF_2)_n$ (n = 2−3) Clusters with Zero and Nonzero Ionic Polarizabilities (ξ) and Average Polarization Energies of Terminal, $E_{pol}(F_t^-)$, and Bridging Fluorides, $E_{pol}(F_b^-)$[a]

system	$E(\xi = 0)$	$E(\xi_{Mg} = 0.7, \xi_F = 2.3)$	$E_{pol}(F_t^-)$	$E_{pol}(F_b^-)$
$(MgF_2)_2$ (D_2h)	−1.613021	−1.629240	26.0×10^{-3}	15.5×10^{-3}
$(MgF_2)_2$ (C_3v)	−1.539264	−1.570661	24.3×10^{-3}	19.5×10^{-3}
$(MgF_2)_3$ (D_2d)	−2.377144	−2.474793	25.8×10^{-3}	15.3×10^{-3}
$(MgF_2)_3$ (C_s)	−2.377174	−2.474665	25.9×10^{-3}	17.0×10^{-3}
$(MgF_2)_3$ (D_3h)	−2.380724	−2.461276	25.6×10^{-3}	4.8×10^{-3}

[a] Atomic units are used throughout.

The PIM introduced in paper I becomes, after these results, a natural model emerging from quantum mechanical simulations in which the behavior of every proper subsystem has been isolated from the rest by the AIM theory. It is simple, quantitative, and in agreement with physical and chemical intuition. We think that large scale realistic simulations of much bigger $(MgF_2)_n$ clusters, out of reach for present ab initio methodologies, are at hand if this interaction model is used. Work along this line is being done in our laboratory.

VI. Conclusions

The equilibrium geometry and vibrational spectra of the less energetic isomers of $(MgF_2)_2$ and $(MgF_2)_3$ clusters have been investigated at the RHF/TZV(1d) and MP2/TZV(1d) theoretical levels. Candidate stable isomers have been selected by means of a Monte Carlo growing strategy that uses simple EGM simulations in order to obtain a multiplicity of guess configurations. The latter are subsequently optimized and ordered in energy, becoming starting geometries for the ab initio minimizations. In this way, we have found that a C_s trimer follows in energy to the known D_{2d} configuration.

Basis set and correlation effects have been found to run parallel to those found for the monomer. Polarization functions are essential to achieve saturation of geometries. The classical correlation among interatomic distances and coordination indices, as well as that between the dissociation energy per molecule and the size of the cluster, is clearly seen even in these small clusters. Our results are in good agreement with the scarce cohesive experimental data when available. A crude statistical calculation shows that the population of the several isomers at high temperatures is not negligible.

An important effort has been made in matching our harmonic vibrational spectra with the disperse, difficult to interpret, spectroscopic measurements. Some reassignments and the ratification of a few definitive bands have been proposed.

The AIM analysis of the wave functions becomes much more fruitful here than in the monomer. All isomers are extremely ionic molecules, and many chemical graphs contain not only cation−anion bonds but also anion−anion bond paths. All bond critical points display density and Laplacian values very similar to those of the monomer, with the differences being directly related to the bond distance variability. The atomic multipoles integrated over the atomic basins have been found to neatly classify the ions according to the coordination index of both cations and anions. We think that this is the germ of the Pauling−Brown rules found in the solid state.

Finally, the polarizable-ions model introduced in our previous work is shown to be a simple, intuitive, and predictive tool to understand the behavior of these systems. We firmly believe that this electrostatic model may be used confidently to study the growth of $(MgF_2)_n$ clusters beyond the sizes amenable to ab initio modeling.

Acknowledgment. We are very grateful to the Spanish Dirección General de Investigación Científica y Técnica (DGICYT), Project No. BQU2000-0466, for financial support. Careful reading of the manuscript by Prof. Lorenzo Pueyo is gratefully acknowledged. We are also very grateful to R. W. F. Bader for providing our group of a copy of the AIMPAC suite of programs.

References and Notes

(1) Berkowitz, J.; Marquart, J. R. *J. Chem. Phys.* **1962**, *37*, 1853.
(2) Lesiecki, M. L.; Nibler, J. W. *J. Chem. Phys.* **1976**, *64*, 871.
(3) Gigli, G. *J. Chem. Phys.* **1990**, *93*, 5224.
(4) Martin, T. P. *J. Chem. Phys.* **1978**, *69*, 2036.
(5) Kim, Y. S.; Gordon, R. G. *J. Chem. Phys.* **1973**, *60*, 4332.
(6) Guido, M.; Gigli, G. *J. Chem. Phys.* **1977**, *66*, 3920.
(7) Ramondo, F.; Bencivenni, L.; Spoliti, M. *J. Mol. Struct. (THEOCHEM)* **1992**, *277*, 171. Spoliti, M.; Bencivenni, L.; Ramondo, F.; Rossi, V. *J. Mol. Struct. (THEOCHEM)* **1994**, *315*, 19.
(8) Ystenes, M.; Westberg, N. *Spectrochim. Acta, Part A* **1995**, *51*, 1501. Ystenes, B. K. *Spectrochim. Acta, Part A* **1998**, *54*, 855.
(9) Simandiras, E. D.; Nicolaides, C. A. *Chem. Phys. Lett.* **1994**, *223*, 233.
(10) Axten, J.; Trachtman, M.; Bock, C. W. *J. Phys. Chem.* **1994**, *98*, 7823.
(11) Rittner, E. S. *J. Chem. Phys.* **1951**, *19*, 1030.
(12) Francisco, E.; Martín Pendás, A.; Costales, A. *J. Phys. Chem.* **2001**, *105*, 4126.
(13) Bader, R. F. W. *Atoms in Molecules;* Oxford University Press: Oxford, U.K., 1990.
(14) Gordon, R. G.; Kim, Y. S. *J. Chem. Phys.* **1972**, *56*, 3122.
(15) Francisco, E.; Recio, J. M.; Blanco, M. A.; Martín Pendás, A.; Pueyo, L. *Phys. Rev. B* **1995**, *51*, 2703.
(16) Phillips, N. G.; Conover, C. W. S.; Bloomfield, L. A. *J. Chem. Phys.* **1991**, *94*, 4980.
(17) McLean, A. D.; Chandler, G. S. *J. Chem. Phys.* **1980**, *72*, 5639.
(18) Dunning, T. H. *J. Chem. Phys.* **1971**, *55*, 716.
(19) Schmidt, M. W.; Baldridge, K. K.; Boatz, J. A.; Elbert, S. T.; Gordon, M. S.; Jensen, J. H.; Koseki, S.; Matsunaga, N.; Nguyen, K. A.; Su, S. J.; Windus, T. L.; Dupuis, M.; Montgomery, J. A. *J. Comput. Chem.* **1993**, *14*, 1347.
(20) Handy, N. C.; Schaefer, H. F., III. *J. Chem. Phys.* **1984**, *81*, 5031.
(21) Frisch, M. J.; Trucks, G. W.; Schlegel, H. B.; Scuseria, G. E.; Robb, M. A.; Cheeseman, J. R.; Zakrzewski, V. G.; Montgomery, J. A., Jr.; Stratmann, R. E.; Burant, J. C.; Dapprich, S.; Millam, J. M.; Daniels, A. D.; Kudin, K. N.; Strain, M. C.; Farkas, O.; Tomasi, J.; Barone, V.; Cossi, M.; Cammi, R.; Mennucci, B.; Pomelli, C.; Adamo, C.; Clifford, S.; Ochterski, J.; Petersson, G. A.; Ayala, P. Y.; Cui, Q.; Morokuma, K.; Malick, D. K.; Rabuck, A. D.; Raghavachari, K.; Foresman, J. B.; Cioslowski, J.; Ortiz, J. V.; Stefanov, B. B.; Liu, G.; Liashenko, A.; Piskorz, P.; Komaromi, I.; Gomperts, R.; Martin, R. L.; Fox, D. J.; Keith, T.; Al-Laham, M. A.; Peng, C. Y.; Nanayakkara, A.; Gonzalez, C.; Challacombe, M.; Gill, P. M. W.; Johnson, B. G.; Chen, W.; Wong, M. W.; Andres, J. L.; Head-Gordon, M.; Replogle, E. S.; Pople, J. A. *Gaussian 98*, revision A.8; Gaussian, Inc.: Pittsburgh, PA, 1998.
(22) Baru, W. H. *Acta Crystallogr.* **1976**, *32*, 2200.
(23) *JANAF Termochemical Tables*, 3rd ed.; Chase, M. W., et al., Eds.; The Dow Chemical Co.: Midland, MI, 1985.
(24) McQuarrie, D. A. *Statistical Mechanics;* Harper & Row: New York, 1976.
(25) Snelson, A. *J. Phys. Chem.* **1966**, *73*, 3028.
(26) Mann, D. E.; Calder, G. V.; Seshadri, K. S.; White, D.; Linevsky, M. J. *J. Chem. Phys.* **1967**, *46*, 1138.
(27) Calder, V.; Mann, D. E.; Seshadri, K. S.; Allavena, M.; White, D. *J. Chem. Phys.* **1969**, *51*, 2093. 26. Hauge, R. H.; Margrave, J. L.; Kana'an, A. S. *J. Chem. Soc., Faraday Trans. 2* **1975**, *71*, 1082.
(28) Francisco, E. et al. To be published.